Bioorganic Chemistry 84 (2019) 202–210

Contents lists available at ScienceDirect

Bioorganic Chemistry

journal homepage: www.elsevier.com/locate/bioorg

Synthesis, molecular modeling and BACE-1 inhibitory study of tetrahydrobenzo[*b*] pyran derivatives

Vijaya Bhaskar[a,*], Reshma Chowdary[b], Sheshagiri R. Dixit[c], Shrinivas D. Joshi[c]

[a] Department of Pharmaceutical Chemistry, Manipal College of Pharmaceutical Sciences, Manipal University, Manipal 576104, India
[b] Department of Medicinal Chemistry, BITS-Pilani Hyderabad Campus, Hyderabad 500078, India
[c] Novel Drug Design and Discovery Laboratory, Department of Pharmaceutical Chemistry, SET's College of Pharmacy, Dharwad 580002, India

ARTICLE INFO

Keywords:
Tetrahydrobenzo [*b*] pyrans
Ionic liquid
1-Butyl-3-imidazolium chloride
β-secretase
Surflex dock
Molecular docking

ABSTRACT

β-Secretase (BACE1) has been broadly documented as one of the possible therapeutic targets for the treatment of Alzheimer's disease. In this paper, we report the synthesis and the for *β*-secretase (BACE-1) inhibitory activity of new series of tetrahydrobenzo [*b*] pyran derivatives. One-pot synthesis of tetrahydrobenzo [*b*] pyrans was carried out by condensing aromatic aldehyde, malononitrile and 1,3-cyclohexanedione using ionic liquid 1-butyl-3-methyl imidazolium chloride ([bmIm]Cl^-) in aqueous alcohol media. The addition of alcohol and water in the ratio of 1:2 keeps all the reactants in solution which facilitates the reaction and makes the product formation very easy. The synthesized compounds were subjected to BACE1 inhibition assay and six compounds, **4d, 4e, 4f, 4h, 4i,** and **4p** have shown significant IC_{50} values at micromolar level. Among these six active compounds, **4e** was a potential inhibitor with its IC_{50} value in nanomolar range. All the synthesized compounds were docked onto the active site of *β*-Secretase enzyme.

1. Introduction

Alzheimer's disease (AD) is one of the neurodegenerative disorders of the central nervous system and most common cause of dementia among old age people. Dementia is a serious brain disorder that affects daily life and activities through loss of memory, cognitive deficits and psychiatric symptoms. It is the fourth major cause of death in the developed world after heart disease, cancer and stroke [1]. Nearly 40 million people worldwide are suffering from AD, out of which 5.5 million are from America and every 70 s someone in America develops the Alzheimer's disease. It is expected that by 2050 this disease will affect 1 in 85 people globally (see Fig. 1).

Presently, a range of methods of treatment are aimed to manage only the symptoms of the disease. No permanent therapy is available for AD patients. The conclusion of the new research says [2–4] that, the deposition of an increased level of amyloid-*β* (A*β*) plaques in the brain over a long period is a leading cause of AD. Amyloid-*β* is produced in neurons from amyloid precursor protein (APP) by the action of an aspartic protease enzyme called *β*-secretase. This enzyme is also known as *β*-site amyloid precursor protein cleaving enzyme1 (BACE 1) or membrane-associated aspartic protease 2 (memapsin-2) or aspartyl protease 2 (Asp2). It is an important enzyme found early in the cascade of biological events leading to the progression of the disease [1,4–12]. A rational research attempt has been made to reduce A*β* levels in the brain and it has become an attractive advance for the development of drugs to curtail AD [13,14].

First identified in 1999, BACE1 belongs to the type-I class of aspartyl proteases. BACE1 is now considered as the favoured therapeutic target for reducing brain A*β* levels in the prevention or treatment of AD.

Till date, no molecule has received FDA approval for the clinical trials. However many molecules have been found with promising clinical potential inhibitory activity. The potentially invented molecules have been classified as peptide-mimetic and non peptidic-inhibitors [15–17]. The research was mainly carried out to investigate for the non-peptide inhibitors with smaller in size, with less peptidic character, better metabolic stability, and also better blood-brain-barrier penetration ability. Many small organic scaffolds have been identified through computational studies which have BACE1 inhibitory activity [5,18–20].

Based on these studies a small attempt has been made to investigate further BACE1 inhibition by using tetrahydrobenzo [*b*] pyran derivatives.

* Corresponding author.
E-mail address: bhaskerkv@gmail.com (V. Bhaskar).

https://doi.org/10.1016/j.bioorg.2018.11.023
Received 3 March 2018; Received in revised form 16 November 2018; Accepted 17 November 2018
Available online 19 November 2018

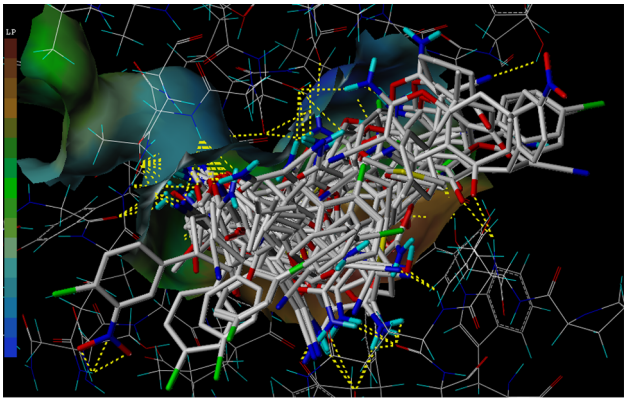

Fig. 1. All molecules docked at the active site of the enzyme PDB ID 4L7G.

2. Results and discussion

2.1. Chemistry

The general procedure for the synthesis of target compounds **4a-4s** and **6a-6t** are given in Schemes 1 and 2 and the list of synthesized compounds are given in Table 2 and 3. The experimental procedure adopted here is very facile and convenient. The attractive features of synthesis by using ionic liquids are simple procedure, short reaction time, excellent yields, room temperature conditions, and easy work-up procedure. This is a one pot, three-component model of cyclo-condensation which involves knoevenagel condensation reaction.

A mixture of an aldehyde, 1, 3-cyclohexanedione (for **4a-4s** compounds) and dimedone (for **6a-6t** compounds) and malononitrile (active methylene compound) was stirred at room temperature in the presence of an ionic liquid, 1-butyl-3-methyl imidazolium Bromide ([bmIm]Br), for a period of 40–60 min based on the type of aromatic aldehyde used. The substituents of aromatic aldehydes affect the reaction times and the yield of products. When aromatic aldehydes with electron-withdrawing groups (such as nitro and halogens) are used the reaction time shorter than with electron-donating groups (such as methoxy and hydroxyl groups). Recrystallization of the crude product from aqueous methanol afforded pure needle shaped crystals of tetrahydrobenzo[*b*]pyrans. The compounds of Scheme 2 were purified by column chromatography using silica.

A variety of substituted aryl and hetero-aryl aldehydes underwent condensation with active methylene compounds (malononitrile) and 1, 3-cyclohexanedione (or dimedone) by this procedure to provide the corresponding 4-aryl substituted tetrahydrobenzo[*b*]pyrans. Their physical and spectral data are discussed as given below.

All these reactions are fast and high yielding (85–95%) compared to the other existing procedures. The recrystallized product gave only a single spot in TLC. Only 0.05 M of catalyst was sufficient for every one

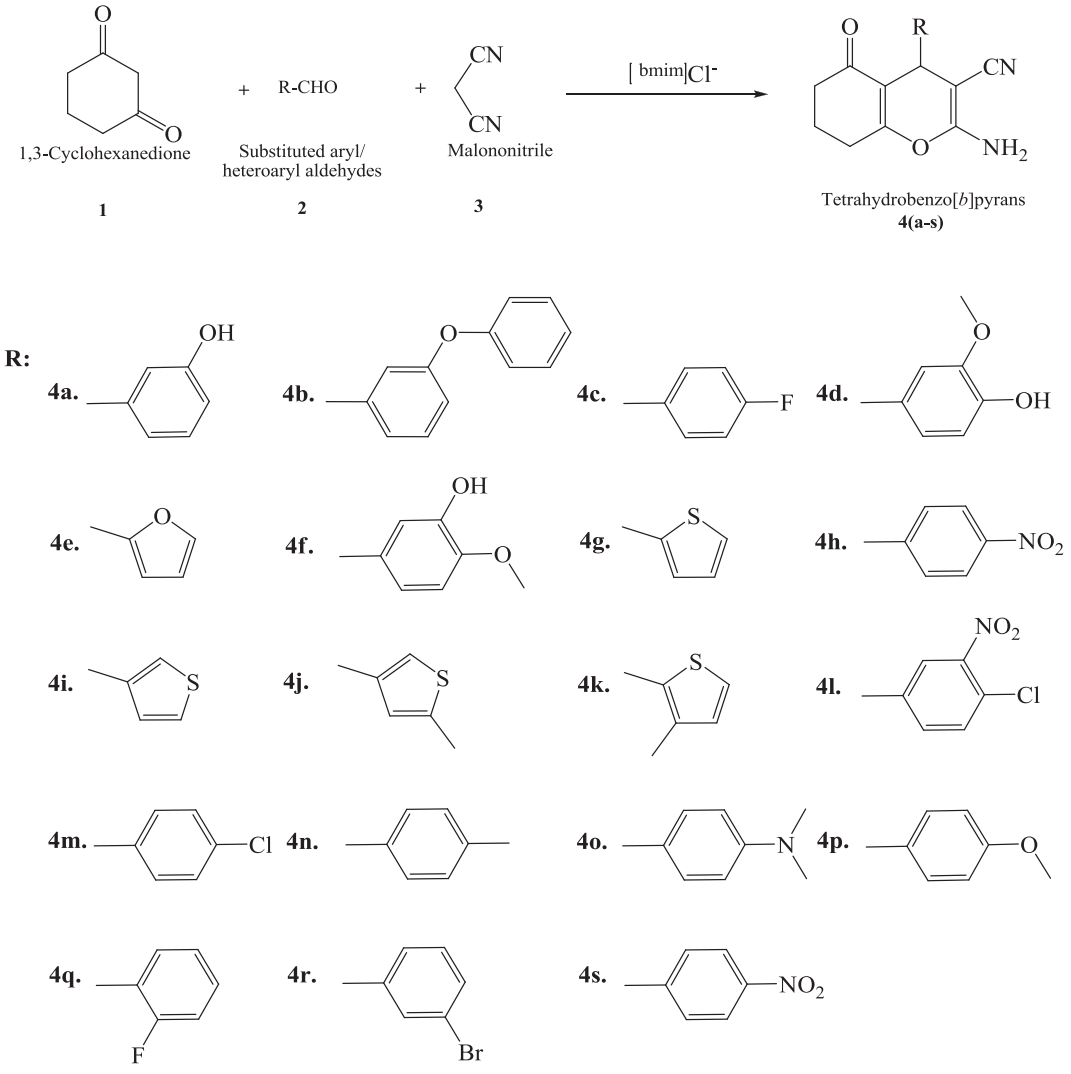

Scheme 1.

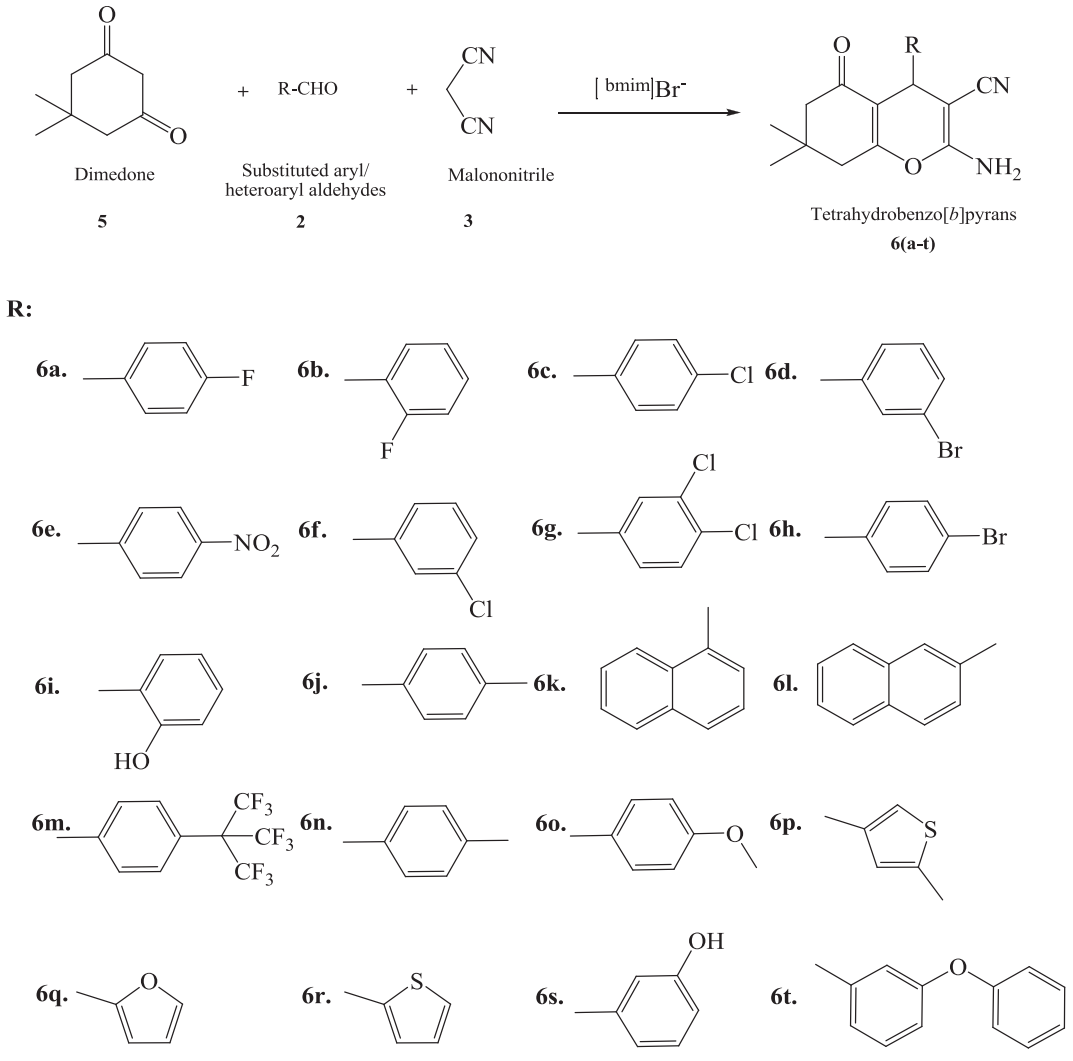

Scheme 2.

molar each of the starting materials. The reaction conditions were mild (only at room temperature) accepting several functional groups, such as $-CH_3$, −F, −Cl, −Br, $-OCH_3$, $-NO_2$, present in molecules. The highly sensitive functional aldehydes like furyl and thienyl (hetero aldehydes) participated in this reaction without any difficulty. All the compounds could be satisfactorily characterized by their spectroscopic (IR, ^1H, ^{13}C NMR) data.

2.2. BACE1 in-vitro assay

The percentage inhibitory activities of all the synthesized compounds obtained by subjecting them to *in-vitro* β-Secretase enzyme inhibition assay are given in Table 5.

Initially, the test was performed at 25 μM concentration for all the compounds. The compounds which showed percentage inhibitions ranging from 65.4 to 98.8% have been considered for further studies. The remaining compounds were ignored due to abnormal results or because of low inhibition.

The compounds which gave percentage of inhibition between 65.4 and 98.8% at 25 μM, were subjected them again for testing at 100 μM, 50 μM, 10 μM, 5 μM, 1 μM, 0.5 μM, 0.1 μM and 0.05 μM. The percentages of inhibition obtained from the above tests have been used to calculate the IC_{50} values. The IC_{50} values were calculated by plotting logarithmic concentration on the x-axis and percentage of inhibition on the y-axis as shown in Fig. 3. Five compounds, **4d, 4f, 4h, 4i** and **4p** were shown IC_{50} values in micro molar level as shown in Table 6 and only one compound **4e** had shown in nano molar level.

2.3. Molecular docking studies

All the conformations were minimized using Tripos force field as shown in Fig. 1. The atomic charges were calculated using MMFF94 (Merck Molecular Force Field) method, while Amber7FF02 was used for the protein. As depicted in Fig. 2, AKB 20 makes four H-bonding interaction with the amino acid ASP228 i.e., Hydrogen of NH_2 at the ortho-position of coumarin ring interacts with oxygen of amino acid ASP228 (H-NH_2———ASP228, 2.24, 2.55, 2.66 and 2.08 Å), nitrogen of CN at the meta-position of coumarin ring makes H-bonding with hydrogen of amino acid THR232 (N-CN————THR232, 2.90 Å) and oxygen of phenoxy ring at the para-position of coumarin ring makes hydrogen bonding with amino acid THR232 (O———THR232, 1.93 Å) The results of molecular docking are listed in Table 1.

3. Experimental

Melting points were determined using Shital-digital programmable melting point apparatus and are uncorrected. FTIR spectra in KBr pellets were recorded on a Bruker FTIR spectrophotometer. The ^1H and ^{13}C NMR spectra were recorded on a Bruker AVANCE II at 400 and 100/75 MHz, respectively; chemical shifts are expressed in parts per million

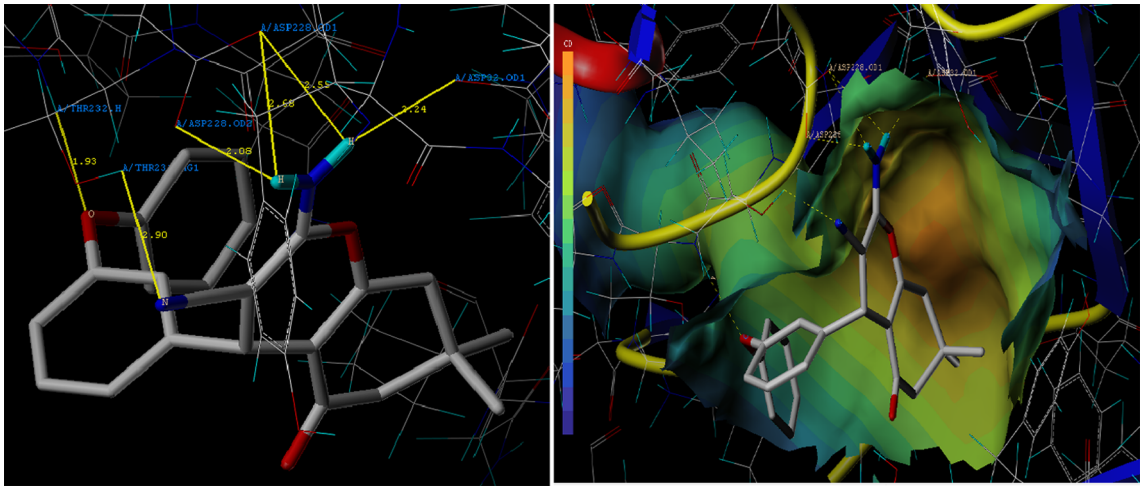

Fig. 2. Docked view of Molecule AKB 20 at the active site of the enzyme (PDB ID: 4L7G).

Table 1
Surflex-Dock scores (kcal/mol) of Tetrahydrobenzo*[b]*pyran.

Compound	C score[a]	Crash score[b]	Polar score [c]	D score[d]	PMF score[e]	G score[f]	Chem score[g]
KVB1	4.38	−0.44	0.96	−105.19	−28.49	−154.82	−22.90
KVB2	2.93	−0.59	0.00	−89.64	−10.92	−136.34	−13.14
KVB3	2.58	−0.71	0.90	−61.63	−18.56	−111.27	−16.32
KVB4	3.74	−0.54	2.09	−81.83	−33.07	−121.75	−23.76
KVB5	2.59	−0.63	0.22	−92.83	−14.46	−138.52	−15.49
KVB6	4.42	−0.51	2.13	−86.98	−26.86	−114.06	−20.54
KVB7	2.42	−0.79	0.98	−84.30	−25.72	−148.45	−21.16
KVB8	2.68	−0.40	1.11	−80.65	−10.32	−121.39	−15.59
KVB9	4.62	−1.26	2.48	−94.99	−47.83	−162.50	−28.58
KVB10	3.45	−0.79	1.34	−88.80	−35.77	−154.35	−20.77
KVB11	2.63	−0.23	1.67	−73.53	−1.75	−98.31	−16.05
KVB12	2.69	−0.61	0.93	−62.63	−15.14	−112.48	−16.16
KVB13	2.69	−2.22	2.00	−96.21	9.21	−174.71	−21.45
KVB14	4.76	−0.98	1.67	−98.33	−43.75	−179.41	−22.22
KVB15	3.47	−0.66	0.04	−92.31	−48.66	−169.49	−21.42
KVB16	4.02	−0.54	2.19	−88.27	−16.44	−135.04	−20.32
KVB17	5.21	−1.14	1.14	−100.12	−53.45	−166.10	−24.00
AKB1	3.35	−0.65	0.83	−87.27	−46.99	−163.05	−20.69
AKB2	3.55	−0.74	1.04	−73.55	2.64	−144.16	−17.15
AKB3	2.83	−0.74	1.04	−75.00	−23.03	−133.66	−19.86
AKB4	2.79	−0.72	1.14	−79.19	−9.81	−148.23	−18.42
AKB5	3.51	−0.27	3.39	−70.47	−56.70	−105.30	−21.77
AKB6	3.90	−0.97	2.07	−76.06	−6.79	−143.49	−20.98
AKB7	3.34	−1.51	2.17	−95.57	−40.19	−156.98	−27.17
AKB8	2.45	−0.71	0.80	−71.89	−21.88	−127.24	−17.99
AKB9	4.13	−0.65	2.14	−75.15	−9.83	−126.28	−20.59
AKB10	4.18	−0.76	0.00	−86.76	−38.99	−162.66	−15.66
AKB11	4.00	−0.20	2.11	−19.44	−22.24	−121.48	−22.66
AKB12	4.71	−0.65	2.22	−91.28	7.29	−149.96	−21.73
AKB13	3.66	−0.43	2.26	−77.75	−3.98	−124.58	−19.68
AKB14	3.54	−0.83	1.04	−74.75	5.37	−143.86	−17.13
AKB15	3.74	−0.56	1.95	−72.62	−47.38	−109.98	−21.48
AKB16	2.97	−0.32	1.39	−82.40	−50.54	−148.48	−20.76
AKB17	2.96	−0.29	1.35	−79.24	−54.62	−145.61	−20.28
AKB18	3.07	−0.47	1.95	−90.13	−17.53	−125.90	−19.77
AKB19	4.21	−1.12	1.11	−93.86	−15.45	−167.24	−22.50
AKB20	6.27	−0.83	2.00	−121.45	−30.34	−192.54	−26.91

[a] C Score (Consensus Score) integrates a number of popular scoring functions for ranking the affinity of ligands bound to the active site of a receptor and reports the output of total score.

[b] Crash-score revealing the inappropriate penetration into the binding site. Crash scores close to 0 are favorable. Negative numbers indicate penetration.

[c] Polar indicating the contribution of the polar interactions to the total score. The polar score may be useful for excluding docking results that make no hydrogen bonds.

[d] D-score for charge and van der Waals interactions between the protein and the ligand (work of Kuntz) [29].

[e] PMF-score indicating the Helmholtz free energies of interactions for protein-ligand atom pairs (Potential of Mean Force, PMF) (work of Muegge and Martin) [30].

[f] G-score showing hydrogen bonding, complex (ligand-protein), and internal (ligand-ligand) energies (work of Willett's group) [31].

[g] Chem-score points for hydrogen bonding, lipophilic contact, and rotational entropy, along with an intercept term (work of Eldridge, Murray, Auton, Paolini, and Mee) [32].

Concentration	KVB 5
100.00	155.000000
50.00	101.000000
25.00	90.500000
10.00	70.400000
5.00	70.200000
1.00	64.200000
0.50	35.000000
0.10	14.000000

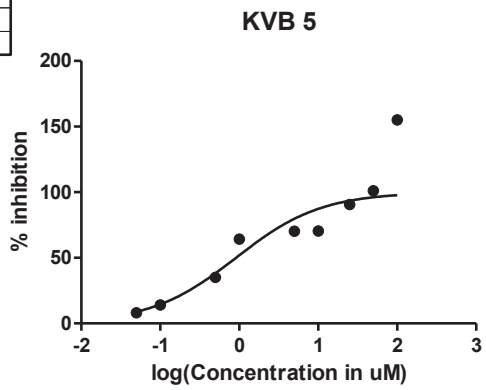

IC50	0.9084

Fig. 3. Calculation of IC50 value of best molecule with a compound code number KVB-5 (4e).

(δ ppm) relative to TMS. The abbreviations used to describe the peak patterns are: (b) broad, (s) singlet, (d) doublet, (t) triplet, (q) quartet, and (m) multiplet (see Fig. 3).

Mass spectra (MS) were recorded in a JEOL GCMATE II GC-Mass spectrometer and Schimadzu QP 20105 GC-Mass spectrometer. Elemental analysis data (performed on Leco Tru Spec CHNS Analyzer) for C, H, and N were all within ± 0.4% of the theoretical values. Analytical thin-layer chromatography (TLC) was performed on the precoated TLC sheets of silica gel 60 F_{254} (Merck, Darmstadt, Germany) visualized by long- and short-wavelength UV lamps. Chromatographic purifications were performed on Merck aluminium oxide (70–230 mesh) and Merck silica gel (70–230 mesh) (see Tables 2–4).

3.1. General procedure for the synthesis of 2-amino-4-substituted-5-oxo-5,6,7,8-tetrahydro-4H-chromene-3-carbonitrile (4a-s) [21]

To mixture of equimolar concentration of substituted aldehydes (5 mmol), malononitrile (5 mmol) and 1, 3-cyclohexanedione (5 mmol), a solution ionic liquid (0.25 mmol) in a 1:1 mixture of water and alcohol was added, the mixture was stirred at room temperature for 24–30 h. The solid separated was filtered off, washed thrice with water (10 ml) and treated with charcoal to remove color impurity and are purified by column chromatography on silica gel with petroleum ether/ethyl acetate (3.5:6.5) as the eluent (see Table 6).

Table 2
The list of compounds prepared from Scheme 1.

Compound	Ar	% Yield	mp (°C)
4a KVB-1	3-hydroxy	85	231
4b KVB-2	3-phenoxy	91	198
4c KVB-3	4-fluro	84	222
4d KVB-4	4-hydroxy, 3-methoxy	89	238
4e KVB-5	2-furyl	82	226
4f KVB-6	3-hydroxy, 4-methoxy	83	218
4g KVB-7	2-Thienyl	81	240
4h KVB-8	4-Nitro	77	229
4i KVB-9	3-thienyl	88	229
4j KVB-10	5-methyl-3-thienyl	77	226
4k KVB-11	3-methyl-2-thienyl	74	230
4l KVB-13	4-chloro, 3-nitro	88	228
4m KVB-14	4-chloro	80	226
4n KVB-15	4-methyl	85	215
4o KVB-16	p-dimethylamino	80	169
4p KVB-17	4-methoxy	85	190
4q KVB-18	2-Fluoro	90	–
4r KVB-19	3-Bromo	88	–
4s KVB-20	4-Nitro	90	–

Table 3
The list of compounds prepared from Scheme 2.

Compound	Ar	% Yield	mp (°C)
6a AKB-1	4-Fluoro	82	274
6b AKB-2	2-Fluoro	75	221
6c AKB-3	4-Chloro	80	210
6d AKB-4	3-Bromo	88	268
6e AKB-5	4-Nitro	86	178
6f AKB-6	3-Chloro	94	222
6g AKB-7	3,4-Dichloro	96	267
6h AKB-8	4-Bromo	86	217
6i AKB-9	2-Hydroxy	88	245
6j AKB-10	4-Methyl	89	214
6k AKB-11	1-Naphthyl	91	245
6l AKB-12	2-Naphthyl	86	224
6m AKB-13	4-Trifluro methyl	87	234
6n AKB-14	H	90	230
6o AKB-15	P-Methoxy	91	201
6p KVB-16	3-Thienyl	88	203
6q AKB-17	2-Furyl	81	220
6r AKB-18	2-Thienyl	78	210
6s AKB-19	3-Hydroxy	65	236
6t AKB-20	3-Phenoxy	86	213

3.1.1. 2-Amino-4-(3-hydroxyphenyl)-5-oxo-5,6,7,8-tetrahydro-4H-chromene-3-carbonitrile (4a)

(Yield 85%). mp 229–231 °C; FTIR (KBr): 3535 (−NH_2), 3369 (−OH), 2185 (−CN, str), 1683 (C═O), 1163 (C−N, str) cm^{-1}; ^{1}H NMR (400 MHz, DMSO) δ ppm: 1.84–1.99 (m, 2H, chromene-C_7-H), 2.22–2.33 (m, 2H, chromene-C_8-H), 2.57–2.60 (t, 2H, chromene-C_6-H), 4.07 (s, 1H, chromene-C_4-H), 6.54–6.57 (m, 3H, ph-C_4, C_6-H and −OH), 6.92 (s, 1H, ph-C_2-H), 7.02–7.06 (t, 1H, ph-C_5-H), 9.25 (s, 2H, −NH_2); ^{13}C NMR (100 MHz, DMSO) δ ppm: 19.76, 26.39, 35.20, 36.28, 58.22, 113.48, 113.93, 113.97, 117.67, 119.72, 129.16, 146.09, 157.23, 158.49, 164.20, 195.70; MS (ESI): m/z = found 281 [$M^+ - 1$]; calcd. 282.29. Anal. Calcd. For $C_{16}H_{14}N_2O_3$: C, 68.07; H, 5.00; N, 9.92. Found: C, 69.75; H, 5.32; N, 10.33.

3.1.2. 2-Amino-5-oxo-4-(3-phenoxyphenyl)-5,6,7,8-tetrahydro-4H-chromene-3-carbonitrile (4b)

(Yield 91%). mp 196–198 °C; FTIR (KBr): 3329–3398 (−NH_2), 2185(−CN, str), 1676 (C═O), 1163 (C−N, str) cm^{-1}; ^{1}H NMR

Table 4
Reaction scheme in biological assay.

Reaction number	1	2	3	4
Assay description	Negative control: no enzyme	Positive control: supplied enzyme activity	Inhibition	Test: sample enzyme activity
Fluorescent assay buffer	80 µl	78 µl	78-X µl	80-Y µl
BACE1 substrate solution, 50 µM	20 µl	20 µl	20 µl	20 µl
BACE1 enzyme solution, 0.3 units/20 µl	–	2 µl	2 µl	–
Inhibitor solution	–	–	X µl	–
Sample enzyme	–	–	–	Y µl
Assay standard solution, 100 µM	–	–	–	–
Total	100 µl	100 µl	100 µl	100 µl

Reaction 1: Negative control reaction with no enzyme is considered as standard curve blank. The "blank" reaction tube reflects fluorescence because of the substrate alone.
Reaction 2: Supplied enzyme – a positive control.
Reaction 3: Enzyme inhibition test.
Reaction 4: Sample enzyme activity test.

1. The fluorescence was noted immediately after adding the enzyme. This is considered as "time zero" reading.
2. The plate was covered with para-filmand incubated at 37 °C for 2 h.

After the "time zero" recording and the next reading was taken after 2 h. The plate was allowed to cool to room temperature before measuring the florescence.

Table 5
The percentage inhibitory activities of all the synthesized compounds obtained by subjecting them to *in-vitro* β-Secretase enzyme inhibition assay are given below.

Compound Code	100 µM	50 µM	25 µM	10 µM	5 µM	1 µM	0.5 µM	0.1 µM	0.05 µM	IC_{50}(µM)
4a	–	–	86.9	103.3	–	–	–	–	–	–
4b	–	–	72.4	11.5	–	–	–	–	–	–
4c	–	–	65.4	32.2	–	–	–	–	–	–
4d	120	99.8	68.8	64.4	61.5	61.4	34.0	12.0	5.0	1.461
4e	155	101	90.5	70.4	70.2	64.2	35.0	14.0	–	0.9084
4f	–	100	98.8	69.9	67.9	1.5	–	–	–	4.042
4g	–	–	102.6	79.1	–	–	–	–	–	–
4h	–	104.6	104.2	95.0	1.6	1.4	–	–	–	7.491
4i	–	102.5	102.5	85.5	1.2	1.3	–	–	–	8.2
4j	–	–	151.7	–	–	–	–	–	–	–
4m	–	–	166.4	–	–	–	–	–	–	–
4n	–	–	66.3	103.8	–	–	–	–	–	–
4o	–	–	170.6	–	–	–	–	–	–	–
4p	–	–	0.7	–	–	–	–	–	–	–
6a	–	–	222.2	–	–	–	–	–	–	–
6b	–	–	23.7	–	–	–	–	–	–	–
6c	–	–	43.1	–	–	–	–	–	–	–
6d	–	–	53.5	–	–	–	–	–	–	–
6e	–	–	41.5	–	–	–	–	–	–	–
6f	–	–	38.7	–	–	–	–	–	–	–
6g	–	–	6.0	–	–	–	–	–	–	–
6h	–	–	-3.9	–	–	–	–	–	–	–
6i	–	–	158.1	–	–	–	–	–	–	–
6j	–	–	10.2	–	–	–	–	–	–	–
6k	–	–	38.7	–	–	–	–	–	–	–
6l	–	–	36.7	–	–	–	–	–	–	–
6m	–	–	76.0	104.7	–	–	–	–	–	–
6n	–	–	55.5	–	–	–	–	–	–	–
6o	–	–	67.8	103.8	–	–	–	–	–	–
6p	–	–	52.2	–	–	–	–	–	–	–
6q	–	100.2	97.3	77.4	1.5	1.6	–	–	–	8.533
6r	–	–	48.1	–	–	–	–	–	–	–
6s	–	–	52.1	–	–	–	–	–	–	–
6t	–	–	38.3	–	–	–	–	–	–	–

Table 6
The calculated IC_{50} values of selected compounds are mentioned in the following table.

Compound	IC_{50} values
4d	1.4610
4e	0.9084
4f	4.0420
4h	7.4910
4i	8.2000
4p	8.5330

(400 MHz, DMSO) δ ppm: 1.80–1.98 (m, 2H, chromene-C_7-H), 2.25–2.30 (m, 2H, chromene-C_8-H), 2.56–2.59 (t, 2H, chromene-C_6-H), 4.17 (s, 1H, chromene-C_4-H), 6.76–6.78 (s, 2H, phenoxy-C_4, C_6-H), 6.90–6.92 (d, 1H, phenoxy-C_2-H), 6.97–7.00 (m, 3H, phenoxy-C_8, C_{10}, C_{12}-H), 7.11–7.15 (t, 1H, phenoxy-C_5-H), 7.25–7.39 (m, 4H, phenoxy-C_9, C_{11}-H and $-NH_2$); ^{13}C NMR (100 MHz, DMSO) δ ppm: 19.00, 26.00, 113.00, 116.00, 118.00, 119.36, 121.00, 129.00, 146.00, 156.00, 158.57, 164.00, 195.35; MS (ESI): *m/z* = found 358 $[M^+ - 1]$; calcd. 358.39. Anal. Calcd. For $C_{16}H_{14}N_2O_3$: C, 68.07; H, 5.00; N, 9.92. Found: C, 69.75; H, 5.32; N, 10.33. GC/MS-*m/z*, 358(M^+281), (M^-35), (M^-63), (M^-81), 246(100).

*3.1.3. 2-Amino-4-(4-fluorophenyl)-5-oxo-5,6,7,8-tetrahydro-4H-chromene-3-carbonitrile (**4c**)*

(Yield 84%). mp 220–222 °C; FTIR (KBr): 3417–3334 (−NH_2), 2191 (−CN str), 1680 (C═O), 1170 (C−N str) cm^{-1}; ^{1}H NMR (400 MHz, DMSO) δ ppm: 1.82–1.98 (m, 2H, chromene-C_7-H), 2.19–2.34 (m, 2H, chromene-C_8-H), 2.54–2.64 (m, 2H, chromene-C_6-H), 4.19 (s, 1H, chromene-C_4-H), 6.98 (s, 2H, ph-C_3, C_5-H), 7.06–7.11 (m, 2H, ph-C_2, C_6-H), 7.15–7.19 (m, 2H, −NH_2); ^{13}C NMR (100 MHz, DMSO) δ ppm: 19.76, 26.39, 35.20, 36.28, 58.22, 113.48, 113.93, 113.97, 119.72, 129.16, 146.09, 157.23, 158.49, 164.20, 195.70. MS (ESI): *m/z* = found 358 [$M^+ - 1$]; calcd. 358.39. Anal. Calcd. For $C_{16}H_{14}N_2O_3$: C, 68.07; H, 5.00; N, 9.92. Found: C, 69.75; H, 5.32; N, 10.33. GC/MS-*m/z*, 222, 189 (100).

*3.1.4. 2-Amino-4-(4-hydroxy-3-methoxyphenyl)-5-oxo-5,6,7,8-tetrahydro-4H-chromene-3-carbonitrile (**4d**)*

(Yield 89%). mp 236-238°C; FTIR(KBr): 3423–3425 (−NH_2), 3327 (Phenolic-OH), 2193 (−CN, str), 1676 (C═O), 1128 (C−N, str) cm^{-1}; ^{1}H NMR (400 MHz, DMSO) δ ppm: 1.81–1.99 (m, 2H, chromene-C_7-H), 2.20–2.33 (m, 2H, chromene-C_8-H), 2.53–2.65 (m, 2H, chromene-C_6-H), 3.29 (s, 3H, −CH_3), 4.08 (s, 1H, chromene-C_4-H), 6.62 (dd, 1H, ph-C_6-H), 6.64–6.67 (t, 2H, ph-C_5-H and −OH), 6.88 (s, 1H, ph-C_2-H), 8.76 (s, 2H, −NH_2); ^{13}C NMR (100 MHz, DMSO) δ ppm:19.00, 26.00, 34.00, 36.00, 114.00, 115.00, 119.00, 135.00, 145.00, 147.55, 158.00, 164.58. MS (ESI): *m/z* = found 358 [$M^+ - 1$]; calcd. 358.39. Anal. Calcd. For $C_{16}H_{14}N_2O_3$: C, 68.07; H, 5.00; N, 9.92. Found: C, 69.75; H, 5.32; N, 10.33. GC/MS-*m/z*, 312 (M^-31), (M^-67), (M^-83), 245(100).

*3.1.5. 2-Amino-4-(furan-2-yl)-5-oxo-5,6,7,8-tetrahydro-4H-chromene-3-carbonitrile (**4e**)*

(Yield 82%). mp 224–226 °C; FTIR (KBr): 3325–3339 (−NH_2), 2187 (−CN str), 1678 (C═O), 1163 (C−N str) cm^{-1}; ^{1}H NMR (400 MHz, DMSO) δ ppm: 1.88–1.96 (m, 2H, chromene-C_7-H), 2.31 (s, 2H, chromene-C_8-H), 2.57 (s, 2H, chromene-C_6-H), 4.31 (s, 1H, chromene-C_4-H), 6.04 (t, 1H, furan-C_4-H), 6.29–6.30 (q, 1H, furan-C_3-H), 7.03 (s, 1H, furan-C_5-H), 7.46 (d, 2H, −NH_2); ^{13}C NMR (100 MHz, DMSO) δ ppm: 19.70, 26.42, 28.94, 36.13, 55.28, 105.04, 110.32, 111.43, 119.48, 141.71, 155.76, 159.25, 165.07, 195.48. MS (ESI): *m/z* = found 358 [$M^+ - 1$]; calcd. 358.39. Anal. Calcd. For $C_{16}H_{14}N_2O_3$: C, 68.07; H, 5.00; N, 9.92. Found: C, 69.75; H, 5.32; N, 10.33. GC/MS-*m/z*, 256 (M^-28), (M^-45), (M^-56), 172 (100).

*3.1.6. 2-Amino-4-(3-hydroxy-4-methoxyphenyl)-5-oxo-5,6,7,8-tetrahydro-4H-chromene-3-carbonitrile (**4f**)*

(Yield 83%). mp 216–218 °C; FTIR (KBr): 3319–3363 (−NH_2), 2191 (−CN str), 1681 (C═O), 1066 (C−N str) cm^{-1}; ^{1}H NMR (400 MHz, DMSO) δ ppm: 1.81–1.99 (m, 2H, chromene-C_7-H), 2.30–2.33 (m, 2H, chromene-C_8-H), 2.56–2.59 (t, 2H, chromene-C_6-H), 4.52 (s, 1H, chromene-C_4-H), 6.83–6.84 (d, 1H, phenyl-C_3-H), 6.88–6.90 (m, 1H, phenyl-C_4-H), 7.08 (s, 2H, NH_2), 7.29–7.30 (t, 1H, phenyl-C_5-H); ^{13}C NMR (100 MHz, DMSO) δ ppm: 20, 26, 30, 36, 58, 114, 120, 124, 127, 149, 159, 164, 196. MS (ESI): *m/z* = found 358 [$M^+ - 1$]; calcd. 358.39. Anal. Calcd. For $C_{16}H_{14}N_2O_3$: C, 68.07; H, 5.00; N, 9.92. Found: C, 69.75; H, 5.32; N, 10.33. GC/MS-*m/z*, 272 (M^-66), 206(100).

*3.1.7. 2-Amino-5-oxo-4-(thiophen-2-yl)-5,6,7,8-tetrahydro-4H-chromene-3-carbonitrile (**4g**)*

(Yield 81%). mp 238–240 °C; FTIR (KBr): 3415–3334 (−NH_2), 2194 (−CN str), 1683 (C═O), 1068 (C−N str) cm^{-1}; ^{1}H NMR (400 MHz, DMSO): δ ppm: 1.81–1.99 (m, 2H, chromene-C_7-H), 2.30–2.33 (m, 2H, chromene-C_8-H), 2.56–2.59 (t, 2H, chromene-C_6-H), 4.52 (s, 1H, chromene-C_4-H), 6.83–6.90 (m, 2H, thiophen-C_3, C_4-H), 7.08 (s, 2H, −NH_2), 7.29–7.30 (t, 1H, thiophene-C_5-H); ^{13}CNMR (100 MHz, DMSO) δ ppm: 20.23, 26.89, 30.80, 36.71, 58.35, 124.41, 124.84, 127.29, 149.73, 159.48, 164.74, 196.14. MS (ESI): *m/z* = found 358 [$M^+ - 1$]; calcd. 358.39. Anal. Calcd. For $C_{16}H_{14}N_2O_3$: C, 68.07; H, 5.00; N, 9.92. Found: C, 69.75; H, 5.32; N, 10.33. GC/MS-*m/z*, 311 (M^-112), 126(100).

*3.1.8. 2-Amino-4-(4-nitrophenyl)-5-oxo-5,6,7,8-tetrahydro-4H-chromene-3-carbonitrile (**4h**)*

(Yield 77%). mp 227–229 °C; FTIR (KBr): 3315–3365 (−NH_2), 2189 (−CN str), 1681 (C═O), 1066 (C−N str) cm^{-1}; ^{1}H NMR (400 MHz, DMSO) δ ppm: 1.84–2.01 (m, 2H, chromene-C_7-H), 2.20–2.35 (m, 2H, chromene-C_8-H), 2.60–2.63 (t, 2H, chromene-C_6-H), 4.35 (s,1H, chromene-C_4-H), 7.13 (s, 2H, ph-C_2, C_6-H), 7.43–7.46 (m, 2H, ph-C_3, C_5-H), 8.13–8.16 (m, 2H, −NH_2); ^{13}C NMR (100 MHz, DMSO) δ ppm: 19.68, 26.47, 35.53, 36.16, 56.87, 112.70, 119.29, 123.58, 128.53, 146.21, 152.26, 158.50, 165.06, 195.81; MS (ESI): *m/z* = found 358 [$M^+ - 1$]; calcd. 358.39. Anal. Calcd. For $C_{16}H_{14}N_2O_3$: C, 68.07; H, 5.00; N, 9.92. Found: C, 69.75; H, 5.32; N, 10.33. GC/MS-*m/z*, 272 (M^-19), (M^-56), (M^-65), 207(100).

*3.1.9. 2-Amino-4-(4-fluorophenyl)-7,7-dimethyl-5-oxo-5,6,7,8-tetrahydro-4H-chromene-3-carbonitrile (**6a**)*

(Yield 82%). mp 272–274 °C; FTIR (KBr): 3313–3358 (−NH_2), 2189 (−CN str), 1680 (C═O), 1151 (C−N str) cm^{-1}; ^{1}H NMR (400 MHz, DMSO) δ ppm: 0.93 & 1.01 (s, 6H, chromene-C_7-H), 2.11 (d, 2H, chromene-C_8-H), 2.25 (t, 2H, chromene-C_6-H), 4.18 (s, 1H, chromene-C_4-CH_3), 6.99–7.17 (m, 4H, ph-C_2, C_3, C_5, C_6-H), 8.29 (s, 2H, −NH_2); ^{13}C NMR (100 MHz, DMSO) δ ppm: 32.37, 37.10, 38.22, 48.90, 112.87, 117.94, 119.30, 130.12, 134.05, 134.14, 149.72, 163.41; MS (ESI): *m/z* = found 358 [$M^+ - 1$]; calcd. 358.39. Anal. Calcd. For $C_{16}H_{14}N_2O_3$: C, 68.07; H, 5.00; N, 9.92. Found: C, 69.75; H, 5.32; N, 10.33. GC/MS-*m/z*, 281(M^-14), 246(100).

*3.1.10. 2-Amino-4-(2-fluorophenyl)-7,7-dimethyl-5-oxo-5,6,7,8-tetrahydro-4H-chromene-3-carbonitrile(**6b**)*

(Yield 75%). mp 219–221 °C; FTIR (KBr): 3327–3398 (−NH_2), 2196 (−CN str),1662 (C═O), 1151 (C−N str) cm^{-1}; ^{1}H NMR (400 MHz, DMSO) δ ppm: 0.95 & 1.03 (s, 6H, chromene-C_7-CH_3), 2.05–2.27 (d, 2H, chromene-C_8-H), 2.43–2.56 (d, 2H, chromene-C_6-H), 4.43 (s, 1H, chromene-C_4-H), 7.00 (s, 2H, −NH_2), 7.07–7.24 (m, 4H, ph-C_3, C_4, C_5, C_6-H); ^{13}C NMR (100 MHz, DMSO) δ ppm: 26.59, 28.45, 31.77, 38.90, 49.88, 56.72, 111.36, 115.49, 119.45, 124.37, 124.41, 128.58, 131.23, 158.73, 161.14, 163.07, 195.53; MS (ESI): *m/z* = found 358 [$M^+ - 1$]; calcd. 358.39. Anal. Calcd. For $C_{16}H_{14}N_2O_3$: C, 68.07; H, 5.00; N, 9.92. Found: C, 69.75; H, 5.32; N, 10.33. GC/MS-*m/z*, 358(M^+281), (M^-35), (M^-63), (M^-81), 246(100).

*3.1.11. 2-Amino-4-(3-chlorophenyl)-7,7-dimethyl-5-oxo-5,6,7,8-tetrahydro-4H-chromene-3-carbonitrile (**6c**)*

(Yield 80%). mp 208–210 °C; FTIR (KBr): 3319–3389 (−NH_2), 2191 (−CN str), 1678 (C═O), 1151 (C−N str) cm^{-1}; ^{1}H NMR (400 MHz, DMSO) δ ppm: 0.96 & 1.04 (s, 6H, chromene-C_7-CH_3), 2.09–2.28 (m, 2H, chromene-C_8-H), 2.51–2.52 (m, 2H, chromene-C_6-H), 4.20 (s, 1H, chromene-C_4-H), 7.05 (s, 1H, ph-C_6-H), 7.19 (d, 2H, ph-C_4, C_5-H), 7.36 (d,1H, ph-C_2-H), 7.99 (m, 2H, −NH_2); ^{13}C NMR (100 MHz, DMSO) δ ppm: 26.85, 31.77, 35.09, 49.93, 57.77, 112.32, 119.50, 128.25, 129.09, 129.71, 131.08, 143.72, 158.48, 162.58, 195.62; MS (ESI): *m/z* = found 358 [$M^+ - 1$]; calcd. 358.39. Anal. Calcd. For $C_{16}H_{14}N_2O_3$: C, 68.07; H, 5.00; N, 9.92. Found: C, 69.75; H, 5.32; N, 10.33. GC/MS-*m/z*, 222, 189 (100).

*3.1.12. 2-Amino-4-(2,4-dichlorophenyl)-7,7-dimethyl-5-oxo-5,6,7,8-tetrahydro-4H-chromene-3-carbonitrile (**6g**)*

(Yield 96%). mp 265–267 °C; FTIR (KBr): 3327–3396 (−NH_2), 2196 (−CN, str), 1658 (C═O), 1149 (C−N str) cm^{-1}; ^{1}H NMR (400 MHz, DMSO) δ ppm: 0.94 & 1.02 (s, 6H, chromene-C_7-CH_3), 2.09–2.25 (m, 2H, chromene-C_8-H), 2.48–2.51 (m, 2H, chromene-C_6-H), 4.23 (s, 1H, chromene-C_4-H), 7.10 (s, 1H, ph-C_6-H), 7.37 (d, 1H, ph-C_5-H), 7.56 (d, 1H, ph-C_3-H), 8.29 (s, 2H, −NH_2); ^{13}C NMR (100 MHz, DMSO) δ ppm:

32.37, 37.10, 48.90, 54.85, 113.03, 119.47, 125.00, 130.54, 134.13, 146.88, 157.17, 163.41, 164.74; MS (ESI): *m/z* = found 358 [M^+-1]; calcd. 358.39. Anal. Calcd. For $C_{16}H_{14}N_2O_3$: C, 68.07; H, 5.00; N, 9.92. Found: C, 69.75; H, 5.32; N, 10.33. GC/MS-*m/z*, 312 (M^-31), (M^-67), (M^-83), 245(100).

*3.1.13. 2-Amino-4-(4-methylphenyl)-7,7-dimethyl-5-oxo-5,6,7,8-tetrahydro-4H-chromene-3-carbonitrile (**6j**)*

(Yield 89%). mp 212–214 °C; FTIR (KBr): 3425–3450 (−NH_2), 2194 (−CN str), 1676 (C═O), 1145 (−C−N str) cm^{-1}; ^{1}H NMR (400 MHz, DMSO) δ ppm: 0.93–1.09 (s, 6H, chromene-C_7-H_3), 2.05–2.09 (m, 2H, chromaene-C_8-H), 2.21–2.25 (t, 2H, chromene-C_6-H), 2.23 (s, 3H, C_4'-H of −CH_3), 4.11 (s, 1H, chromene-C_4-H), 6.88–6.90 (dd, 1H, phenyl-$C_{3'}$, $C_{5'}$-H), 6.93 (s, 2H, −NH_2), 7.06–7.08 (dd, 1H, phenyl-$C_{2'}$, $C_{6'}$-H); ^{13}C NMR (100 MHz, DMSO) δ ppm: 20.56, 31.00, 35.00, 37.00, 49.00, 113.00, 118.00, 120.00, 124.00, 125.00, 129.00, 130.00, 149.58, 163.00. MS (ESI): *m/z* = found 358 [M^+-1]; calcd. 358.39. Anal. Calcd. For $C_{16}H_{14}N_2O_3$: C, 68.07; H, 5.00; N, 9.92. Found: C, 69.75; H, 5.32; N, 10.33. GC/MS-*m/z*, 256 (M^-28), (M^-45), (M^-56), 172 (100).

*3.1.14. 2-Amino-7,7-dimethyl-4-(naphthalen-1-yl)-5-oxo-5,6,7,8-tetrahydro-4H-chromene-3-carbonitrile (**6k**)*

(Yield 91%). mp 243–245 °C; FTIR (KBr): 3325–3454 (−NH_2), 2194 (−CN str), 1666 (C═O), 1136 (C−N str) cm^{-1}; ^{1}H NMR (400 MHz, DMSO) δ ppm: 1.01 & 1.07 (s, 6H, chromene-C_7-CH_3), 2.06–2.27 (2d, 2H, chromene-C_8-H), 2.60 (d, 2H, chromene-C_6-H), 5.16 (s, 1H, chromene-C_4-H), 6.96 (s, 1H, naphthyl-C_2-H), 7.26 (d, 1H, naphthyl-C_3-H), 7.44–7.59 (m, 3H, naphthyl-C_4, C_6, C_7-H), 7.79 (d, 1H, naphthyl-C_5-H), 7.94 (d, 1H, naphthyl-C_8-H), 8.40 (d, 2H, −NH_2); ^{13}C NMR (100 MHz, DMSO) δ ppm: 26.97, 30.25, 31.81, 38.90, 50.00, 58.92, 113.43, 119.60, 123.59, 125.79, 126.94, 128.36, 130.74, 133.32, 141.91, 158.42, 162.73, 195.68. MS (ESI): *m/z* = found 358 [M^+-1]; calcd. 358.39. Anal. Calcd. For $C_{16}H_{14}N_2O_3$: C, 68.07; H, 5.00; N, 9.92. Found: C, 69.75; H, 5.32; N, 10.33. GC/MS-*m/z*, 272 (M^-66), 206(100).

*3.1.15. 2-Amino-7,7-dimethyl-4-(naphthalen-2-yl)-5-oxo-5,6,7,8-tetrahydro-4H-chromene-3-carbonitrile (**6l**)*

(Yield 86%). mp 222–224 °C; FTIR (KBr): 3313–3350 (NH_2), 1147 (C−N str), 2189 (−CN str), 1680 (C═O) cm^{-1}; ^{1}H NMR (400 MHz, DMSO) δ ppm: 0.95 & 1.03 (s, 6H, chromene-C_7-CH_3), 2.05–2.27 (2d, 2H, chromene-C_8-H), 2.48–2.54 (m, 2H, chromene-C_6-H), 7.03 (s, 1H, naphthyl-C_1-H), 7.28 (dd, 3H, naphthyl-C_3, C_5, C_6-H), 7.43–7.50 (m, 2H, naphthyl-C_4, C_8-H), 7.65 (s, 1H, naphthyl-C_7-H), 7.82–7.88 (m, 2H, −NH_2); ^{13}C NMR (100 MHz, DMSO): 26.74, 31.79, 35.87, 49.99, 58.12, 112.54, 119.68, 125.62, 126.15, 127.41, 127.62, 128.07, 131.98, 132.83, 142.00, 158.48, 162.54, 195.69; MS (ESI): *m/z* = found 358 [M^+-1]; calcd. 358.39. Anal. Calcd. For $C_{16}H_{14}N_2O_3$: C, 68.07; H, 5.00; N, 9.92. Found: C, 69.75; H, 5.32; N, 10.33. GC/MS-*m/z*, 311 (M^-112), 126(100).

*3.1.16. 2-Amino-4-(3-hydroxyphenyl)-7,7-dimethyl-5-oxo-5,6,7,8-tetrahydro-4H-chromene-3-carbonitrile (**6s**)*

(Yield 65%). mp 234–236 °C; FTIR (KBr): 3311–3454 (NH_2), 3315 (−OH), 2198 (−CN str), 1676 (C═O), 1151 (C−N str) cm^{-1}; ^{1}H NMR (400 MHz, DMSO) δ ppm: 0.95 & 1.03 (s, 6H, chromene-C_7-CH_3), 2.47–2.49 (m, 2H, chromene-C_6-H), 4.05 (s, 1H, chromene-C_4-H), 6.53–6.56 (m, 3H, −OH & ph-C_4, C_6-H), 6.94 (s, 1H, ph-C_2-H), 7.06 (t, 1H, ph-C_5-H), 9.28 (s, 2H, −NH_2); ^{13}C NMR (100 MHz, DMSO) δ ppm: 26.78, 31.77, 35.43, 49.98, 58.39, 112.87, 113.54, 114.09, 119.73, 129.18, 146.12, 157.28, 158.51, 162.31, 195.56.

*3.1.17. 2-Amino-7,7-dimethyl-5-oxo-4-(3-phenoxyphenyl)-5,6,7,8-tetrahydro-4H-chromene-3-carbonitrile (**6t**)*

(Yield 86%). mp 211–213 °C; FTIR (KBr): 3331–3379 (−NH_2), 2191 (−CN str), 1681 (C═O), 1153 (C−N str) cm^{-1}; ^{1}H NMR (400 MHz, DMSO) δ ppm: 0.90 & 1.01 (s, 6H, chromene-C_7-CH_3), 2.07–2.26 (2d, 2H, chromene-C_8-H), 2.39–2.53 (m, 2H, chromene-C_6-H), 4.16 (s, 1H, chromene-C_4-H), 6.74 (s, 1H, phenoxy-C_4-H), 6.81 (dd, 1H, phenoxy-C_6-H), 6.90–6.99 (M, 4H, phenoxy-C_2, C_8, C_{10}, C_{12}-H), 7.14 (t, 1H, phenoxy-C_5-H), 7.26–7.38 (m, 4H, −NH_2 and naphthyl-C_9, C_{11}-H); ^{13}C NMR (400 MHz, DMSO) δ ppm: 26.70, 28.43, 31.70, 35.40, 49.92, 57.99, 112.36, 116.54, 117.12, 118.59, 119.56, 122.18, 123.45, 129.97, 146.96, 156.37, 156.63, 158.47, 162.64, 195.58; MS (ESI): *m/z* = found 358 [M^+-1]; calcd. 358.39. Anal. Calcd. For $C_{16}H_{14}N_2O_3$: C, 68.07; H, 5.00; N, 9.92. Found: C, 69.75; H, 5.32; N, 10.33. GC/MS-*m/z*, 272 (M^-19), (M^-56), (M^-65), 207(100).

3.2. Biological screening studies

3.2.1. BACE1 in-vitro assay

The BACE1 inhibitory assay was carried out by using β-Secretase activity detection kit purchased from Sigma-Aldrich Company, USA. The kit is provided with all the necessary reagents, along with the BACE1 enzyme to be used as a positive control, which is required for the detection of BACE1 inhibitory activity. The assay is based on the principle of fluorescence resonance energy transfer (FRET) in which the fluorescence signal enhancement is observed after the substrate is cleaved by BACE1.

The principle of the assay of BACE1 involves the synthesis of the peptide substrate with the help of two fluorophores, Viz., fluorescent donor and a proprietary quenching acceptor. The distance between these two groups has been assigned, so that upon light excitation, the donor fluorescence energy is significantly quenched by the acceptor through a phenomenon known as resonance energy transfer. Upon cleavage by the protease, the fluorophore will be separated from the quenching group, restoring the full fluorescence yield of the donor. Thus, a weak fluorescent peptide substrate becomes highly fluorescent upon enzymatic cleavage; the increase in fluorescence is linearly related to the rate of proteolysis [19,22]. The assay was performed in duplicate on all the compounds.

Equipment and reagents required

- Fluorometer
- Well plate for fluorescence assay
- Dimethyl sulfoxide (DMSO)

Procedure

1. The fluorometer was set on well plate reader mode with excitation at 320 nm and emission at 405 nm.
2. All the components were brought (except the BACE1 enzyme solution) to the room temperature.
3. All the components were added to a fluorometer 96 well plate according to the following regimen. It was thoroughly mixed. The BACE1 enzyme was added just before reading.

3.2.2. Assay of BACE1 inhibitors

Enzyme activity inhibition reactions were set using reactions 1–3 (blank, enzyme activity reaction, and inhibition reaction) as described in Table 4. Reaction 3 was expanded to include a few wells with different concentrations of the inhibitor ([Asn670, Sta671, Val672]-Amyloid β/A4 Precursor Protein 770 Fragment 662–675) and this reaction which was performed at 37 °C for 2 h.

3.3. Molecular docking studies

Molecular docking studies were carried out [23] using the Sybyl-X, version 2.0, run on a Intel® CoreTM i3-2130 CPU @ 3.40 GHz processor on a Windows-7 professional workstation. When docking was performed with default settings, it revealed a number of possible conformations and orientations for the inhibitors at the binding site. Understanding of the binding site conformations helped us to understand

the important interactions that could stabilize ligand-receptor complex. Surflex-Dock adopted the empirical scoring function using the patented searching engine [24,25] for molecular docking. The crystal structure of Diethylaminosulfur trifluoride-mediated intramolecular cyclization of 2-hydroxy-benzylureas to Fused bicyclic amino oxazoline compounds and evaluation of their biochemical activity against Beta-Secretase-1 (BACE1) was selected from the Protein Data Bank ((PDB entry code 4L7G) extracted from the Brookhaven Protein Database http://www.rcsb.org/pdb) and these were used in the initial docking. Co-crystallized ligand and water molecules were removed from the structure, while the essential hydrogen atoms were added and side chains were fixed during the protein preparation. The 3D structures of pyrrole derivatives were constructed using the standard geometric parameters of Sybyl-X 2.0 software and the structure was subjected to energy minimization. The MMFF94 (Merk Molecular Force Field) charges were calculated for the ligand, while Amber7FF02 was used for the protein. The model was then subjected to energy minimization following the gradient termination of Powell method for 3000 iterations using the Tripos force field [26] with non-bonding cut-off value set at 8.0 and dielectric constant set at 1.0. Then, ligand-based docking was introduced to generate the “protomol”, and all the inhibitors were docked within the prepared protein. In order to identify the ligand-protein interactions, the top pose and protein were loaded into the work area and MOLCAD (Molecular Computer Aided Design) program was employed to visualize the binding mode between the protein and the ligand. MOLCAD calculates and exhibits the surfaces of channels and cavities as well as separating surface between the protein subunits [27,28]. MOLCAD program provides to create molecular surface by using fast Connolly method, a marching cube algorithm to engender the surface.

Acknowledgements

We thank, Dr. Akkattu T Biju, Scientist from NCL, Pune, for all his guidance and support in synthesis of compounds. We are also thankful for Dr. D. Sriram, Professor from BITS, Hyderabad, for his help in biological screening and finally we are extremely thankful to Principal, Manipal College of Pharmaceutical Sciences, Manipal, for supporting in accomplishing this project.

References

[1] J. Hardy, D. Allsop, Amyloid deposition as the central event in the aetiology of Alzheimer's disease, Trends Pharmacol. Sci. 12 (1991) 383–388.
[2] A. Goate, J. Hardy, Twenty years of Alzheimer’s disease-causing mutations, J. Neurochem. 120 (s1) (2012) 3–8.
[3] R. Yan, et al., Membrane-anchored aspartyl protease with Alzheimer's disease β-secretase activity, Nature 402 (6761) (1999) 533–537.
[4] C. Haass, D.J. Selkoe, Soluble protein oligomers in neurodegeneration: lessons from the Alzheimer's amyloid β-peptide, Nat. Rev. Mol. Cell Biol. 8 (2) (2007) 101–112.
[5] A.K. Ghosh, H.L. Osswald, BACE1 (β-secretase) inhibitors for the treatment of Alzheimer's disease, Chem. Soc. Rev. 43 (19) (2014) 6765–6813.
[6] P.C. Kandalepas, R. Vassar, Identification and biology of β-secretase, J. Neurochem. 120 (s1) (2012) 55–61.
[7] H. Zhang, et al., Proteolytic processing of Alzheimer’s β-amyloid precursor protein, J. Neurochem. 120 (s1) (2012) 9–21.
[8] F. Checler, A.J. Turner, Journal of Neurochemistry special issue on Alzheimer’s disease: ‘amyloid cascade hypothesis–20 years on’, J. Neurochem. 120 (s1) (2012) iii–iv.
[9] R. Vassar, et al., β-Secretase cleavage of Alzheimer's amyloid precursor protein by the transmembrane aspartic protease BACE, Science 286 (5440) (1999) 735–741.
[10] C. Morgan, et al., Structure and function of amyloid in Alzheimer's disease, Prog. Chem. Org. Nat. Prod. Neurobiol. 74 (6) (2004) 323–349.
[11] A. Mudher, S. Lovestone, Alzheimer's disease–do tauists and baptists finally shake hands? Trends Neurosci. 25 (1) (2002) 22–26.
[12] C. Reinhard, S.S. Hébert, B. De Strooper, The amyloid-β precursor protein: integrating structure with biological function, EMBO J. 24 (23) (2005) 3996–4006.
[13] A.K. Ghosh, S. Gemma, J. Tang, β-Secretase as a therapeutic target for Alzheimer's disease, Neurotherapeutics 5 (3) (2008) 399–408.
[14] B. De Strooper, R. Vassar, T. Golde, The secretases: enzymes with therapeutic potential in Alzheimer disease, Nat. Rev. Neurol. 6 (2) (2010) 99–107.
[15] S. Hanessian, et al., Structure-based design, synthesis, and memapsin 2 (BACE) inhibitory activity of carbocyclic and heterocyclic peptidomimetics, J. Med. Chem. 48 (16) (2005) 5175–5190.
[16] E. Viayna, et al., Synthesis and multitarget biological profiling of a novel family of rhein derivatives as disease-modifying anti-Alzheimer agents, J. Med. Chem. 57 (6) (2014) 2549–2567.
[17] Y. Shimmyo, et al., Flavonols and flavones as BACE-1 inhibitors: structure–activity relationship in cell-free, cell-based and in silico studies reveal novel pharmacophore features, Biochim. Biophys. Acta (BBA)-General Subjects 1780 (5) (2008) 819–825.
[18] S.S. Madhukar, et al., In silico design of inhibitors for-secretase: implications for Alzheimer's Disease, Curr. Trends Biotechnol. Pharm. 7 (1) (2013) 558–566.
[19] Y. Niu, et al., The discovery of novel β-secretase inhibitors: pharmacophore modeling, virtual screening, and docking studies, Chem. Biol. Drug Des. 79 (6) (2012) 972–980.
[20] A.K. Ghosh, et al., Structure-based design: potent inhibitors of human brain memapsin 2 (β-secretase), J. Med. Chem. 44 (18) (2001) 2865–2868.
[21] K. Gong, et al., One-pot synthesis of polyfunctionalized pyrans catalyzed by basic ionic liquid in aqueous media, J. Heterocycl. Chem. 46 (6) (2009) 1145–1150.
[22] M.E. Kennedy, et al., Measuring human β-secretase (BACE1) activity using homogeneous time-resolved fluorescence, Anal. Biochem. 319 (1) (2003) 49–55.
[23] Tripos International, Sybyl-X 2.0, Tripos International, St. Louis, MO, USA, 2012.
[24] A.N. Jain, Scoring noncovalent protein-ligand interactions: a continuous differentiable function tuned to compute binding affinities, J. Comput. Aided Mol. Des. 10 (1996) 427–440.
[25] A.N. Jain, Surflex: fully automatic flexible molecular docking using a molecular similarity-based search engine, J. Med. Chem. 46 (2003) 499–511.
[26] M. Clark, R.D. Cramer, V.N. Opdenbosch, Validation of the general purpose tripos 5.2 force field, J. Comput. Chem. 10 (1989) 982–1012.
[27] Y. Ai, S.T. Wang, P.H. Sun, F.J. Song, Molecular modeling studies of 4,5-dihydro-1*H*-pyrazolo[4,3-*H*] quinazoline derivatives as potent CDK2/cyclin a inhibitors using 3D-QSAR and docking, Int. J. Mo. Sci. 11 (2010) 3705–3724.
[28] P. Lan, W.N. Chen, W.M. Chen, Molecular modeling studies on imidazo[4,5-*b*] pyridine derivatives as Aurora A kinase inhibitors using 3D-QSAR and docking approaches, Eur. J. Med. Chem. 46 (2011) 77–94.
[29] I.D. Kuntz, J.M. Blaney, S.J. Oatley, R. Langridge, T.E. Ferrin, A geometric approach to macromolecule-ligand interactions, J. Mol. Biol. 161 (1982) 269–288.
[30] I. Muegge, Y.C. Martin, A general and fast scoring function for protein-ligand interactions: a simplified potential approach, J. Med. Chem. 42 (1999) 791–804.
[31] G. Jones, P. Willett, R. Glen, A.R. Leach, R. Taylor, Development and validation of a genetic algorithm for flexible docking, J. Mol. Biol. 267 (1997) 727–748.
[32] M.D. Eldridge, C.W. Murray, T.R. Auton, G.V. Paolini, R.P. Mee, Empirical scoring functions: I. The development of a fast empirical scoring function to estimate the binding affinity of ligands in receptor complexes, J. Comp. Aided Molec. Des. 11 (1997) 425–445.